Effects of mutations in helix h28 of 16S rRNA on translation initiation in E. coli Undergraduate Research Thesis

Presented in Partial Fulfillment of the Requirements for graduation “with Honors Research Distinction in Microbiology” in the undergraduate colleges of The Ohio State University

By Alexis Dunning

The Ohio State University May 2016

Project Advisor: Dr. Kurt Fredrick, Department of Microbiology

Abstract

16S ribosomal RNA is the main structural and functional component of the 30S ribosomal subunit. During initiation, the 30S subunit binds three protein factors, mRNA and initiator tRNA, and then associates with the 50S subunit. The 30S contains a large "head" domain connected to the remainder of the subunit by the "neck" helix h28. Helix 28 is formed by base pairing between highly conserved nucleotides 921-933 and 1384-1396, and stabilized by interactions with helices h36 and h37. Previous studies have indicated that the structural conformation of the 30S subunit is flexible, specifically about the neck. Formation of the initiation complex appears to involve conformational changes of the head, but the role of these movements in the initiation process remains unclear. To investigate the role of the neck, we created single-nucleotide substitutions in h28 and compensatory mutations that restore the base pairs using site-directed mutagenesis. The effect these mutations have on translation fidelity was analyzed using a *lacZ* reporter gene with cognate (AUG) and near cognate (AUC) start codons. It was found that certain single mutations decreased translation substantially, whereas double mutations that generate alternative base pairs had comparatively small effects. Structural models of 16S rRNA suggest that the most deleterious substitutions disrupt complex tertiary interactions. These results show that the structure of h28 is critical for translation and define the relative importance of specific nucleotides.

Introduction

Translation is the process of synthesizing proteins, which is catalyzed by ribosomes. Ribosomes are composed of two subunits—the large 50S subunit and a smaller 30S subunit. The 30S subunit, the subject of this study, is composed of 16S ribosomal RNA (rRNA) and 20 proteins. The structure of the 30S is characterized as having a head and body domain separated by the neck. During the first phase of translation, initiation, the 30S subunit binds three initiation factors (IF1, IF2, and IF3), followed by binding of the messenger RNA (mRNA) which allows the initiator tRNA to bind the P site. A study by Berk *et al.* illustrated that before the 50S subunit can bind the 30S subunit, steric clash between the initiator tRNA and the central 50S protuberance must be diminished. To eliminate this clash, the 30S subunit tilts its head domain toward the central protuberance of the 50S

subunit, allowing the initiator tRNA to dock in the P-site cleft of the 50S. This allows the 50S to dock onto the 30S, leading to formation of the 70S initiation complex, which is competent to enter the elongation phase. Additionally, the closing of the P-site cleft stabilizes interactions between the mRNA and ribosome, which may prevent mRNA shifting.

Previous studies by Qin *et al* identified specific 30S subunit mutations that increase translation with near cognate start codon AUC. One of these mutations, C1389U, is localized to helix 28 (h28), which corresponds to the neck helix of the 16S rRNA (Figure 1). Other studies have indicated h28 may play a role in 30S head tilting during elongation, specifically aiding in ribosomal translocation (Noller *et al*., 2014) as well as during 50S docking in initiation as previously mentioned (Berk *et al*., 2006; Hickerson *et al*., 2005).

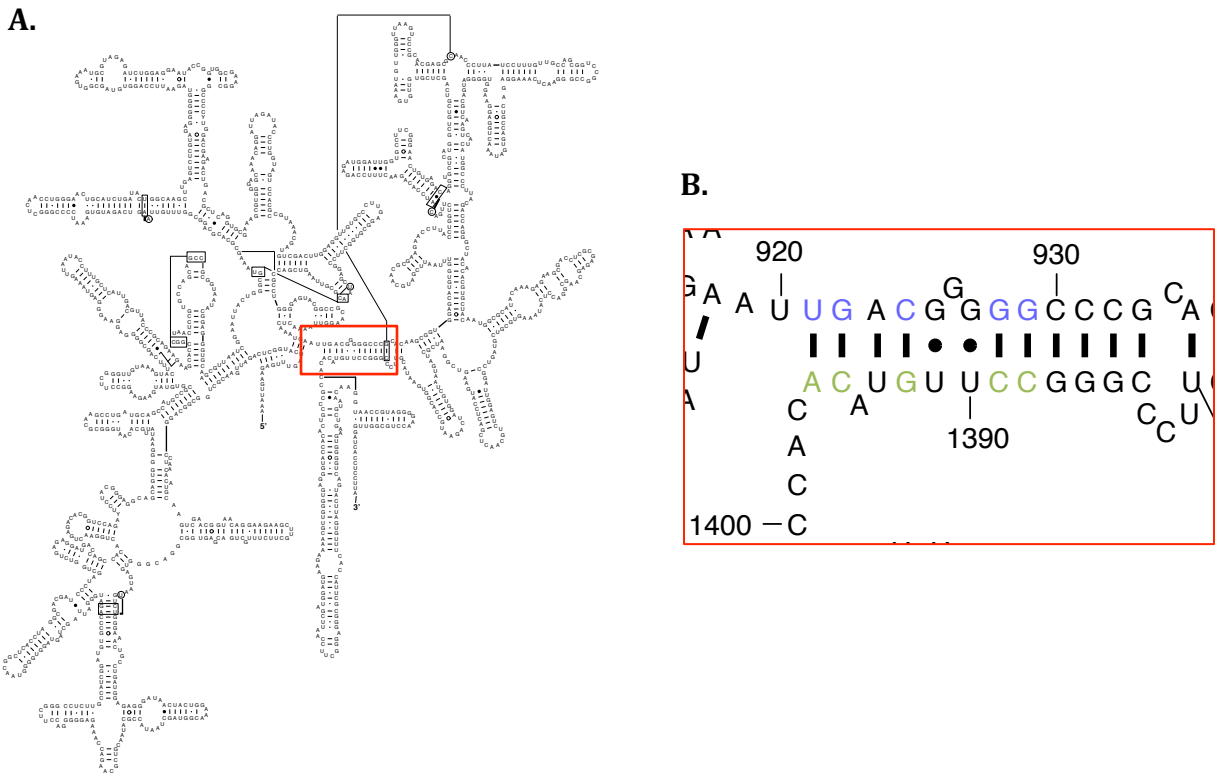

Figure 2. 16S rRNA Secondary Structure and h28 mutation positions.

A. The secondary structure of 16S rRNA, which along with 20 proteins makes up the 30S subunit. The neck region (h28) is boxed in red.
B. Neck region of h28 of the 16S rRNA. Transition mutations were made for top strand positions 921, 922, 924, 928, 929 (in blue) and at bottom strand positions 1396, 1395, 1392, 1389, 1388 (in green). Black lines indicate Watson-Crick pairs, while dots indicate structurally distinct wobble pairs.

Here, we created multiple h28 mutations, which target the highly conserved neck region of 16S rRNA. The effect of these mutations on translation was quantified to elucidate the role of specific positions and nucleotides in translation initiation and fidelity.

Methods

Specialized Ribosome System

To determine the effects on translation, a specialized ribosome system was employed using indicator strains KLF 2674 and KLF 2672. KLF 2674 contains the cognate start codon AUG while KLF 2672 contains the near cognate AUC start codon. Each strain contains the *lacZ* gene with a specialized Shine-Dalgarno (SD*) sequence, 5' ATCCC 3'. The *lacZ* gene is under control of the constitutive P_{ant} promoter and the corresponding mRNA is specifically translated by specialized ribosomes with the anti Shine-Dalgarno (ASD*) sequence 5' GGGGU 3'. To introduce mutant ribosomes into strain KLF 2674 and 2672, plasmid pKF207 was used. The 16S rRNA with complementary ASD* sequence is encoded on pKF207. The transcription of this 16S rRNA is under control by the arabinose inducible P_{BAD} promoter. Ribosomes with unaltered ASD sequences were present in each strain to sustain normal cellular processes (Figure 2).

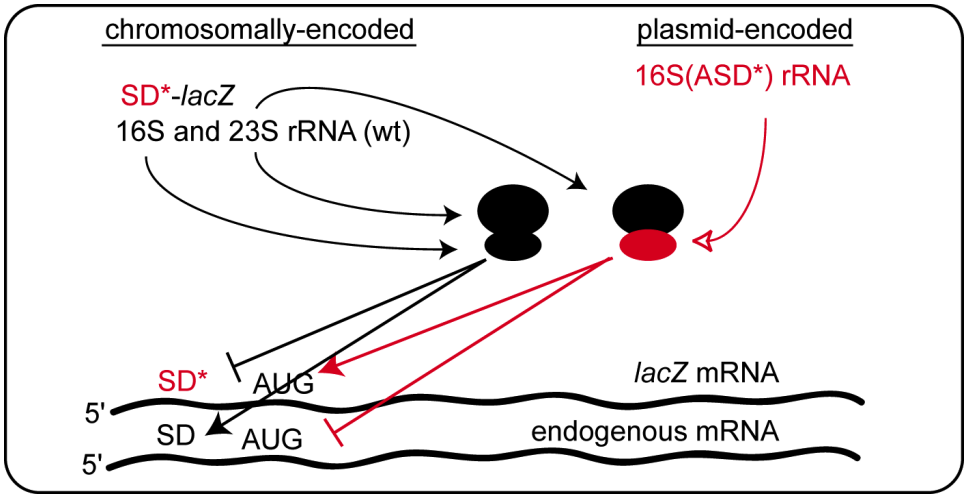

Figure 2. Specialized Ribosome System. The chromosome encodes for the *lacZ* gene with a specialized Shine-Dalgarno sequence (SD*). The mRNA for this gene is only translated by 70S ribosomes containing specialized 30S subunits (in red) with the complementary ASD* sequence. All other mRNAs in the cell are translated by endogenous ribosomes (in black). Mutations were generated in the plasmid encoding the specialized 16S(ASD*) rRNA.

Site Directed Mutagenesis of pKF207 16S rRNA

h28 mutations on the 16S rRNA gene of pKF207 were created using Quikchange and Phusion mutagenesis (Figure 1). Single point mutations generated were as follows: T921C, G922A, C924T, G928A, G929A, A1396G, C1395T, G1392A, C1389T, C1388T. Double mutations, T921C and A1396G, G922A and C1395T, C924T and G1392A, G928A and C1389T, G929A and C1388T, were created through Quikchange and Phusion mutagenesis of already-mutated pKF207. Primers used for mutagenesis are as follows:

T921C Forward: 5' TTAAAACTCAAATGAATCGACGGGGGCCCGCAC 3'
Reverse: 5' GTGCGGGCCCCCGTCGATTCATTTGAGTTTTAA 3'

G922A Forward: 5' TAAAACTCAAATGAATTAACGGGGGCCCGCACAAG 3'
Reverse: 5' CTTGTGCGGGCCCCCGTTAATTCATTTGAGTTTTA 3'

C924T Forward: 5' AAACTCAAATGAATTGATGGGGGCCCGCACAAG 3'
Reverse: 5' CTTGTGCGGGCCCCCATCAATTCATTTGAGTTT 3'

G927A Forward: 5' CAAATGAATTGACGGGAGCCCGCACAAGCGGTG 3'
Reverse: 5' CACCGCTTGTGCGGGCTCCCGTCAATTCATTTG 3'

G928A Forward: 5' CAAATGAATTGACGGGGACCCGCACAAGCGGTG 3'
Reverse: 5' CACCGCTTGTGCGGGTCCCCGTCAATTCATTTG 3'

C1389T Forward: 5' AATACGTTCCCGGGCTTTGTACACACCGCCC 3'
Reverse: 5' GGGCGGTGTGTACAAAGCCCGGGAACGTATT 3'

C1388T Forward: 5' GAATACGTTCCCGGGTCTTGTACACACCGCC 3'
Reverse: 5' GGCGGTGTGTACAAGACCCGGGAACGTATTC 3'

G1392A Forward: 5' ATACACACCGCCCGTCACAC 3'
Reverse: 5' AAGGCCCGGGAACGTATTCA 3'

C1395T Forward: 5' TACACCGCCCGTCACACC 3'
Reverse: 5' TACAAGGCCCGGGAACGTATTC 3'

A1396G Forward: 5' GCACCGCCCGTCACACC 3'
Reverse: 5' GTACAAGGCCCGGGAACGT 3'

Mutant plasmids were transformed into KLF 2674 and KLF 2672 strains. Specific mutations were confirmed following plasmid purification from KLF 2674 and sequencing using primers #1194 (mutations in 900 kb region), and #1594 (mutations in 1300 kb region).

Translation Activity of Mutant Ribosomes

All transformed KLF 2674 and 2672 strains with singly and doubly mutated pKF207 were plated on Luria-Broth plates with ampicillin (100 μg /mL), kanamycin (30 μg/mL), L-arabinose (5 mM), and X-gal (20 μg/mL). The color of each strain was compared to the wild type (KLF 2674 with pKF207 and KLF 2672 with pKF207). KLF 2674 strains generally appeared blue while KLF 2672 strains appear white because of decreased translation activity due to near cognate start codon. To assess the translation activity of mutant ribosomes in vivo, β−Galactosidase assays were used. 10 μL of dense culture of each mutant strain was diluted in 5 mL of Luria Broth containing ampicillin (100 μg/mL), kanamycin (30 μg/mL), and L-arabinose (0.2%) and grown for 6 hours at 37°C. Cells were washed in Z buffer (61 mM Na_2HPO_4, 39 mM NaH_2PO_4, 10 mM KCl, 10 mM $MgSO_4$, pH 7.0) and resuspended in working buffer (Z buffer with 400 nM DTT). Cells were lysed using B-PER (Pierce). ONPG (4 mg/mL in Z buffer) was used as the initial substrate but was not sensitive enough to provide distinguishable results between mutant and wild type strains. CPRG, chlorophenol red-β-D-galactopyranoside, (1 mg/mL in Z buffer) was used in the assays reported here. A_{573} of the lysed sample and OD_{600} of the original cell suspension were measured and used to calculate the specific activity (SA) units. These were defined by $SA = [1000 \bullet A_{573}]/[t \bullet v \bullet OD_{600}]$, where A_{573} is absorbance at 537 nm, t is the reaction time, v is volume of cells used in the reaction (here 0.1 or 0.5 mL), OD_{600} is the absorbance at 600 nm. Six independent experiments were conducted and mean specific activity unit is illustrated here. Student's t-test was performed to determine which apparent differences are statistically significant. Statistical outliers were removed based on Grubbs outlier test as referenced in Statistical Methods (Snedecor and Cochran 278-281).

Results and Discussion

All KLF 2674 (AUG start) strains with mutations in h28, except for three, have significant decreases in translation activity when compared to wild type as seen in Figure 3. The

greatest decreases in translation are seen in strains with mutations G922A, G928A, and G929A. The single mutation C1389U, and double mutations G928A/C1389U and G922A/C1388U do not cause significant decreases in translation.

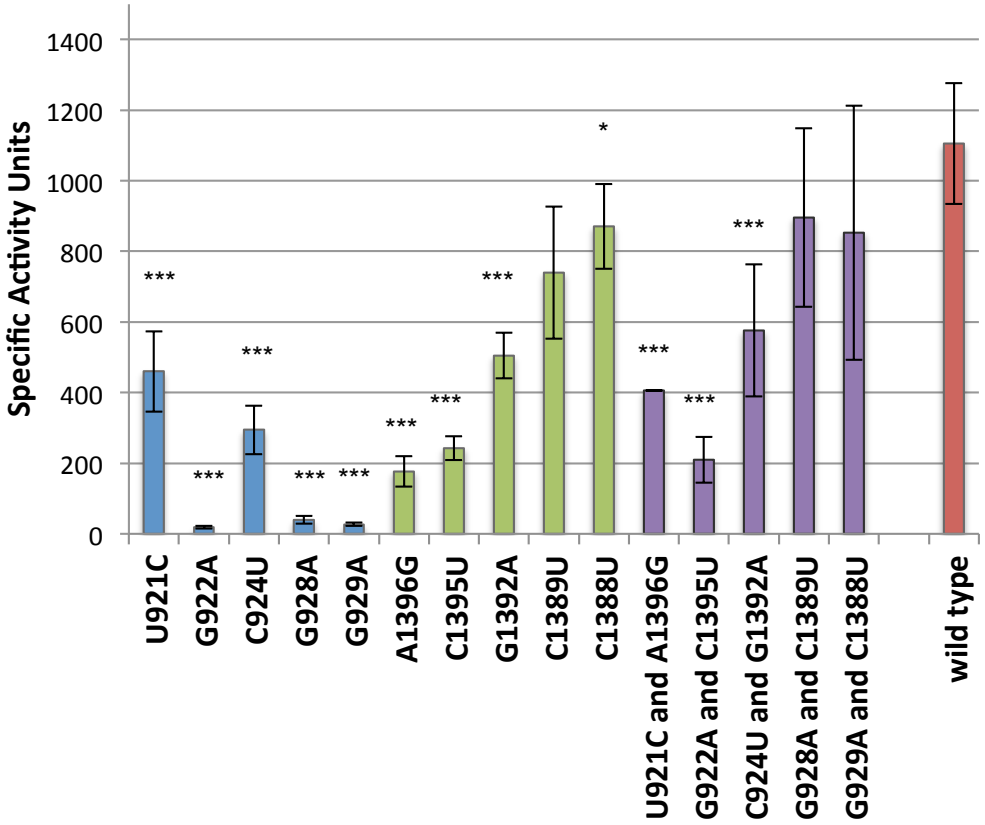

Figure 3. Effects of 16S rRNA h28 mutations on the relative translation activity in KLF 2674 strains (SD*-AUG-*lacZ*). Data obtained from β−galactosidase assays with CPRG and represents mean ± SEM where n ≥ 4. (***, **, * corresponds to uncorrected p values of < 0.001, < 0.01, < 0.05 respectively). Top strand single mutations in blue, bottom strand single mutations in green, and double mutations (i.e. base pair changes) in purple.

Translation activity of mutated KLF 2672 (AUC start) was also measured and compared to the wild type as seen in Figure 4. All strains display decreases in translation activity when compared to the mutant AUG start codon strains, as expected due to the near cognate start codon. Half of the mutant KLF 2672 strains have significant decreased translation activity when compared to wild type. Similar to the AUG case, mutations G922A, G928A, and G929A have the greatest decrease in translation activity from AUC. However, one strain with mutation C1389U has a significant increase in translation. Qin *et al* previously showed this

same result through genetic screens of random 16S rRNA mutant strains on X-gal plates. Colonies with 16S rRNA mutation C1389U was one of 18, which displayed a blue color, indicating increased translation of mRNA's (with AUC start) by these mutant ribosomes. It was inferred that this phenotype is related to altered head dynamics but the precise mechanisms remains vague. A more comprehensive analysis of h28 nucleotides that contribute to initiation fidelity initiated by this work, may help clarify the role of head dynamics in initiation.

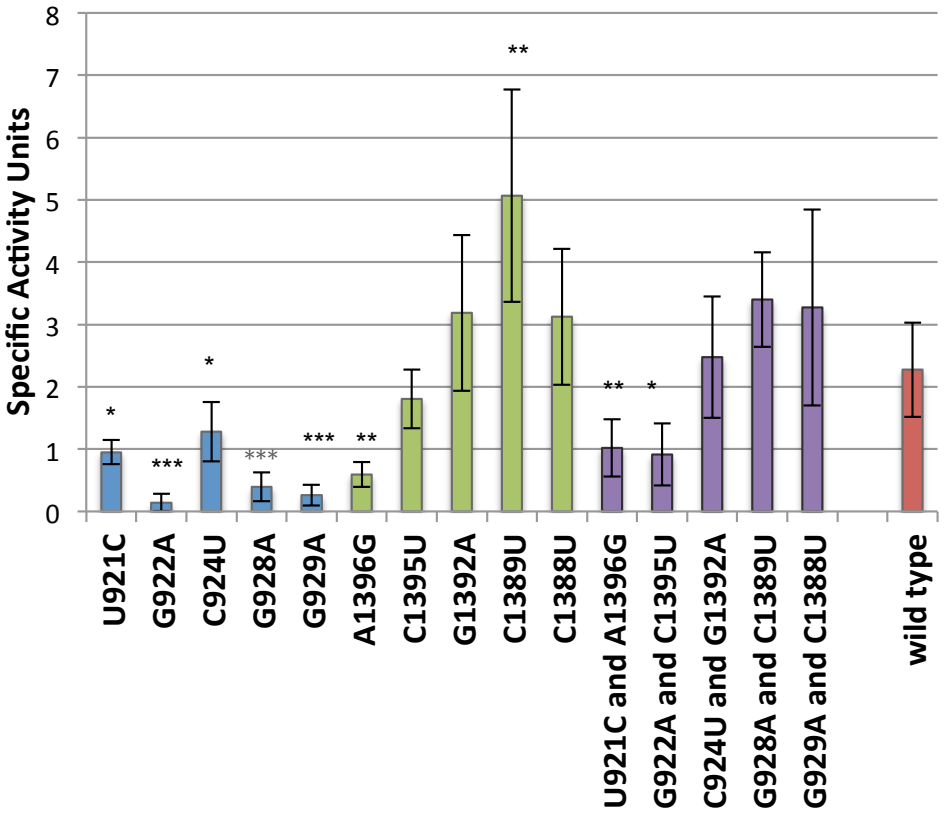

Figure 4. Effects of 16S rRNA h28 mutations on the relative translation activity in KLF 2672 strains (SD*-AUC-*lacZ*). Data obtained from β−galactosidase assays with CPRG and represents mean ± SEM where n ≥ 4. (***, **, * corresponds to uncorrected p values of < 0.001, < 0.01, < 0.05 respectively). Top strand single mutations in blue, bottom strand single mutations in green, and double mutations (i.e. base pair changes) in purple.

To determine the frequency of spurious translation initiation at various h28 positions, the level of β−galactosidase from KLF 2674 relative to KLF 2672 was analyzed (Figure 5). G928A, G929A, C1395U, G1392A, C1389U, C924U/G1392A and G928A/C1389U all exhibit decreased translation initiation fidelity compared to the wild type. Although, the

magnitude of the fidelity defects are generally reduced when base pairing in h28 is restored. The large number of mutations in this region implicates a role of head movement during translation initiation. However, the exact role of nucleotides would require further studies of the mutant ribosomes.

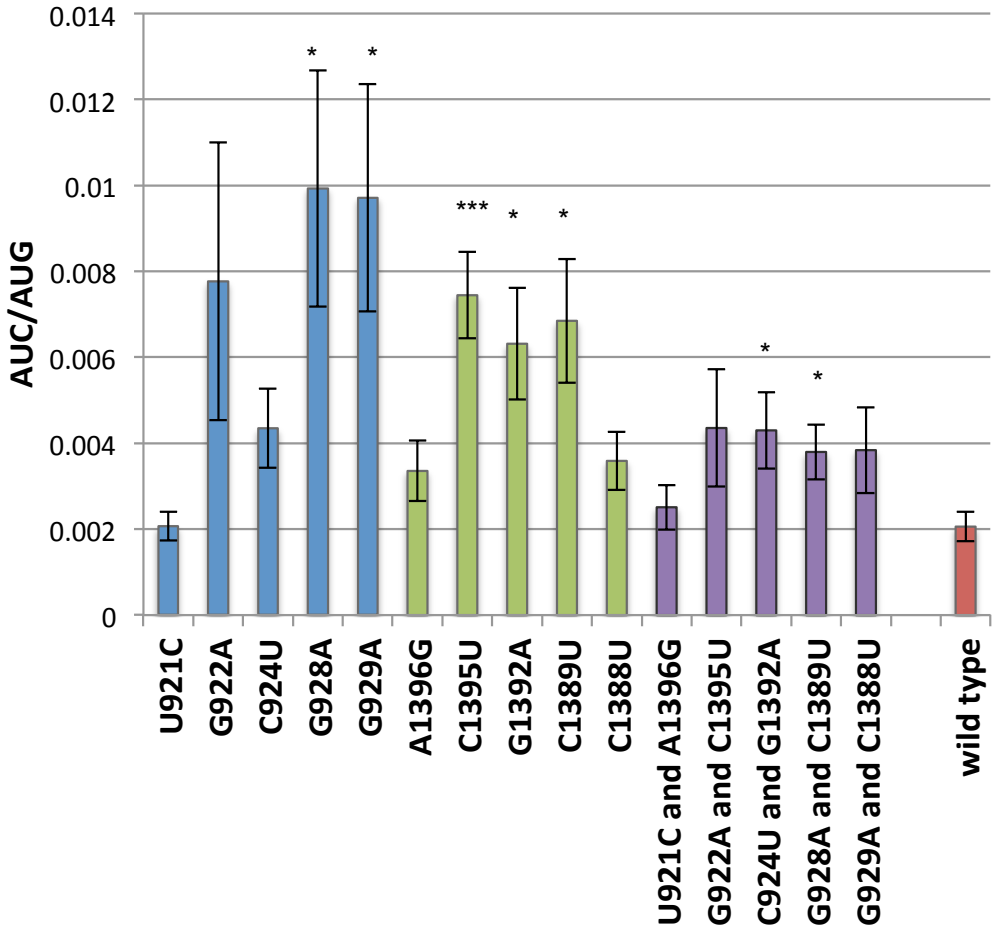

Figure 5. Effects of 16S rRNA h28 mutations on initiation fidelity by examining KLF 2672 strains (SD*-AUC-*lacZ*) translation activity relative to KLF 2674 strains (SD*-AUG-*lacZ*). Data obtained from β−galactosidase assays with CPRG and represents mean ± SEM where n ≥ 4. (***, **, * corresponds to uncorrected p values of < 0.001, < 0.01, < 0.05 respectively). Top strand single mutations in blue, bottom strand single mutations in green, and double (i.e. base pair changes) mutations in purple.

Structural Analysis of U921C, G922A, and C924U

In order to explain the effects seen on translation, an inspection of the structural environment of the targeted nucleotides was conducted. In the typical structure of the 30S subunit, U921, G922, and C924 all engage in tertiary interactions with proteins or other nucleotides (Figure 6). When such interactions are lost due to a mutation, translation

activity in all cases decreases. In the case of the C924U mutation, base pairing within h28 is retained due to the G1392-U924 wobble pairing. However, translation activity is still decreased, indicating the importance of the Watson-Crick pair at this position, which might facilitate specific interactions with A1502. Additionally, G922A exhibits one of the greatest decreases in translation activity. Therefore, its interaction with A1398 must also be important in translation.

A. **B.** **C.**

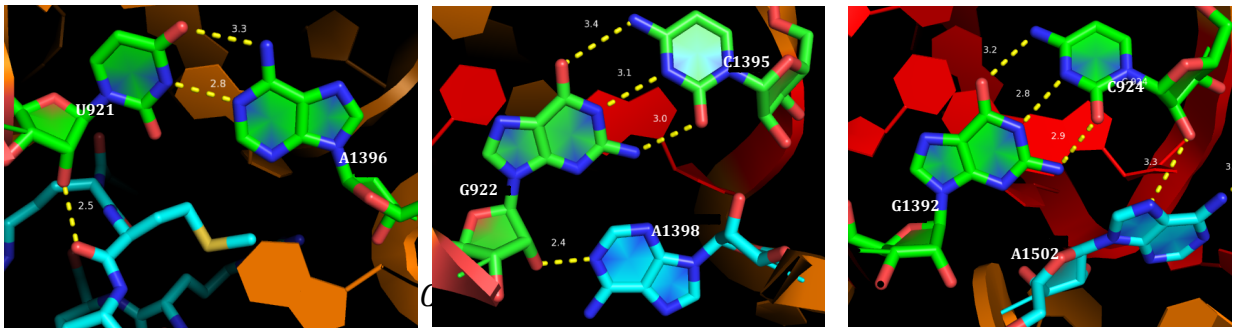

Figure 6. Tertiary structure representation of h28 of 16S rRNA

A. U921-A1396. 2' OH of U921 (green) interacts with S5 protein (light blue)
B. G922-C1395. 2' OH of G922 (green) interacts with nitrogen of A1398 (light blue)
C. C924-G1392. 2' OH of C924 (green) interacts with nitrogen of A1502 (light blue)

Due to the secondary structure of the neck region, single mutations were created independently on each strand (Figure 2). Located on the bottom strand of the neck, A1396, C1395, and G1392 do not engage in tertiary interactions in the typical 30S structure like their corresponding top strand nucleotides do (Figure 6). Therefore, when there is a base substitution in these positions, the bases that typically engage in tertiary interactions are still present. However, in all three mutants, translation activity decreased. A1396 and C1395 can form G-U wobble pairs; however, the shifting of the helix to form these pairs likely disrupts the tertiary interactions involving U921-S5 and G922-A1398 respectively. Upon examination of the 30S secondary structure (Figure 2), the loss of base pairing between G1392 and C924 may cause destabilization of the G-U wobble pair at positions 1391 and 925. This might lead to further separation of the two h28 strands resulting in the loss of C924-A1502 interaction, which could cause the decrease in translation activity in the G1392A mutant.

Structural Analysis of Compensatory Mutations

Double mutations were created to restore base pairing within h28 to determine the role of secondary structure. U921C/A1396G and C924U/G1392A compensatory mutations do not rescue translation activity to wild type levels. This indicates that in this region of h28, the specific nucleotides and their tertiary interactions are more important than the secondary structure. However, in the case of U922C/A1396G when base pairing is restored between the two strands of h28, translation activity increases by 10 fold when compared to G922A strain and by 2 fold when compared to the A1396G strain. Wild type translation activity is not observed in this mutant strain, indicating a possible role of specific nucleotides at these positions. But the large increase in translation activity does point to the importance of secondary structure at these positions as well. This role of base pairing of h28 also may be important in the cases of G928A/C1389U and G929A/C1388U.

G928A and G292A display two of the greatest decreases in translation activity. Upon structural examination, neither nucleotide engages in tertiary interactions with proteins or other nucleotides besides typical base pairing in h28 (Figure 7).

A. **B.**

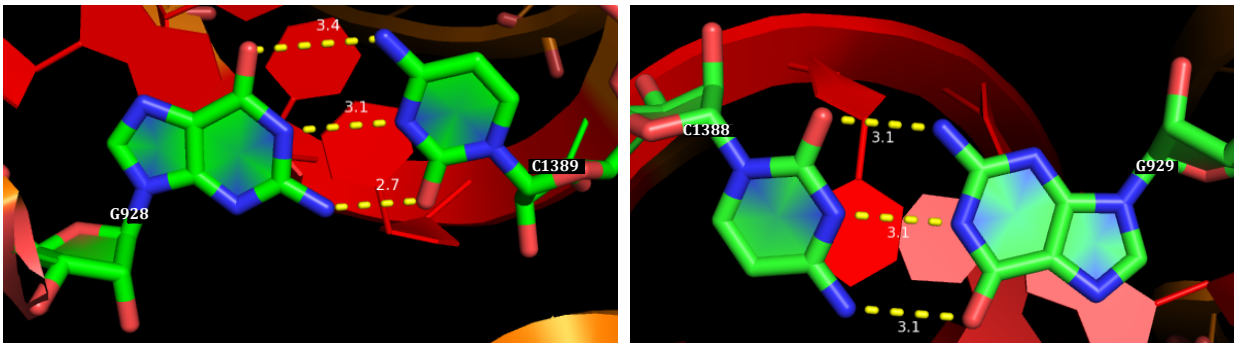

Figure 7. Tertiary structure representation of h28 of 16S rRNA
A. Base pairing between positions G928-C1389
B. Base pairing between positions G929-C1388

The introduction of mutations G928A and G929A caused a loss of local structure. When this structure is partially restored by G-U wobble pairs in the case of C1389U and C1388U, translation activity is rescued by nearly 18 and 45 fold respectively. Additionally, when compensatory mutations are created (G928A/C1389U and G929A/C1388U), translation

activity is also restored to the level of wild type. Therefore, in this region of h28, the local base pairing structure is much more important than the specific nucleotides involved.

Conclusions:

Overall, the data presented here indicate a role of the h28 neck region in translation and translation initiation. Most of the nucleotides and secondary structure of this region appear to play an important role in this process. However, positions 922, 928, 929, and 1389 seem to be the most important due to the tertiary interactions of specific nucleotides at these positions as well as base pairing between the two h28 strands. While the exact involvement of these positions in unclear, further studies will need to be conducted using the mutant ribosomes designed here.

References:

Berk, V., W. Zhang, R. D. Pai, and J. H. D. Cate. "Structural Basis for MRNA and TRNA Positioning on the Ribosome." *Proceedings of the National Academy of Sciences* 103.43 (2006): 15830-5834. Web.

Hickerson, Robyn, Zigurts K. Majumdar, Albion Baucom, Robert M. Clegg, and Harry F. Noller. "Measurement of Internal Movements within the 30S Ribosomal Subunit Using Förster Resonance Energy Transfer." *Journal of Molecular Biology* 354.2 (2005): 459-72. Web.

Mcclory, Sean P., Aishwarya Devaraj, Daoming Qin, Joshua M. Leisring, and Kurt Fredrick. "Mutations in 16S RRNA That Decrease the Fidelity of Translation." *Ribosomes* (2011): 237-47. Web.

Mohan, Srividya, John Paul Donohue, and Harry F. Noller. "Molecular Mechanics of 30S Subunit Head Rotation." *Proceedings of the National Academy of Sciences Proc Natl Acad Sci USA* 111.37 (2014): 13325-3330. Web.

Snedecor, George W., and William G. Cochran. *Statistical Methods*. Ames, IA: Iowa State UP, 1967. Print.

Qin, Daoming, and Kurt Fredrick. "Control of Translation Initiation Involves a Factor-induced Rearrangement of Helix 44 of 16S Ribosomal RNA." *Molecular Microbiology* 71.5 (2009): 1239-249. Web.